PROFESSOR FERRUH ARTUNC (Orcid ID : 0000-0002-3777-9316)

Article type : Regular Paper

Plasminogen deficiency does not prevent sodium retention in a genetic mouse model of experimental nephrotic syndrome

Mengyun Xiao[1], Bernhard N. Bohnert[1-3], Hande Aypek[4], Oliver Kretz[4], Florian Grahammer[4], Ute Aukschun[5], Matthias Wörn[1], Andrea Janessa[1], Daniel Essigke[1], Christoph Daniel[6], Kerstin Amann[6], Tobias B. Huber[4], Edward F. Plow[7], Andreas L. Birkenfeld[1-3], Ferruh Artunc[1-3]

[1] Department of Internal Medicine, Division of Endocrinology, Diabetology and Nephrology, University Hospital Tübingen, Germany

[2] Institute of Diabetes Research and Metabolic Diseases (IDM) of the Helmholtz Center Munich at the University Tübingen, Germany

[3] German Center for Diabetes Research (DZD) at the University Tübingen, Germany

[4] III. Department of Medicine, University Medical Center Hamburg-Eppendorf, Hamburg, Germany

[5] IV. Department of Medicine, Faculty and University Medical Center Freiburg, Freiburg, Germany

[6] Institute of Nephropathology, Friedrich-Alexander University Erlangen-Nürnberg (FAU), Germany

[7] Lerner Research Institute, Cleveland Clinic, Ohio, USA

Address for correspondence:
Ferruh Artunc, MD
University hospital Tübingen
Department of Internal Medicine
Otfried-Mueller-Str.10
72076 Tübingen, Germany
E-mail: ferruh.artunc@med.uni-tuebingen.de
Tel. +49-7071-2982711 / Fax +49-7071-2925215

Short title: Plasminogen and nephrotic syndrome

Abstract

Aim: Sodium retention is the hallmark of nephrotic syndrome (NS) and mediated by the proteolytic activation of the epithelial sodium channel (ENaC) by aberrantly filtered serine proteases. Plasmin is highly abundant in nephrotic urine and has been proposed to be the principal serine protease responsible for ENaC activation in NS. However, a proof of the essential role of plasmin in experimental NS is lacking.

Methods. We used a genetic mouse model of NS based on an inducible podocin knockout (Bl6-Nphs2$^{tm3.1Antc}$*Tg(Nphs1-rtTA*3G)^{8Jhm}*Tg(tetO-cre)^{1Jaw} or *nphs2$^{\Delta ipod}$*). These mice were crossed with plasminogen deficient mice (Bl6-Plg^{tm1Jld} or plg$^{-/-}$) to generate double knockout mice (*nphs2$^{\Delta ipod}$*plg$^{-/-}$*). NS was induced after oral doxycycline treatment for 14 days and mice were followed for subsequent 14 days.

Results. Uninduced *nphs2$^{\Delta ipod}$*plg$^{-/-}$* mice had normal kidney function and sodium handling. After induction, proteinuria increased similarly in both *nphs2$^{\Delta ipod}$*plg$^{+/+}$* and *nphs2$^{\Delta ipod}$*plg$^{-/-}$* mice. Western blot revealed urinary excretion of plasminogen and plasmin in *nphs2$^{\Delta ipod}$*plg$^{+/+}$* mice which was absent in *nphs2$^{\Delta ipod}$*plg$^{-/-}$* mice. After onset of proteinuria, amiloride-sensitive natriuresis was increased compared to the uninduced state in both genotypes. Subsequently, urinary sodium excretion dropped in both genotypes leading to an increase in body weight and development of ascites. Treatment with the serine protease inhibitor aprotinin prevented sodium retention in both genotypes.

Conclusions. This study shows that mice lacking urinary plasminogen are not protected from ENaC-mediated sodium retention in experimental NS. This points to an essential role of other urinary serine proteases in the absence of plasminogen.

Key words: epithelial sodium channel - nephrotic syndrome - plasminogen — proteasuria -sodium retention

Introduction

Nephrotic syndrome (NS) is characterized by heavy proteinuria and sodium retention leading to expansion of extracellular volume and edema formation. Substantial evidence has emerged that aberrantly filtered serine proteases resulting in proteasuria cause sodium retention in NS by activating the epithelial sodium channel (ENaC) through proteolysis of its γ-subunit [1-3]. This is supported by our recent finding that treatment with the serine protease inhibitor aprotinin prevents sodium retention in mice with experimental NS [4]. The serine protease plasmin has been identified as the most abundant serine protease in urine samples of nephrotic rats using affinity chromatography with aprotinin. This led to the hypothesis that plasmin might be the principal serine protease responsible for ENaC activation in NS [5, 6]. Following aberrant filtration of the zymogen plasminogen (plg), plasmin is formed by urokinase-type plasminogen activator (uPA), which is expressed in the tubular epithelium [7-9]. Urine from nephrotic rats and purified plasmin has been shown to increase amiloride-sensitive whole-cell currents in *Xenopus laevis* oocytes heterologously expressing ENaC [5, 10-12]. In patients with proteinuric kidney disease including those with NS, active plasmin was found in the urine and shown to correlate with extracellular volume and overhydration measured by bioimpedance spectroscopy [10]. These findings suggest a pathophysiological role of plasmin in sodium retention of humans with NS although the effects cannot be dissected from the effects of proteinuria and albuminuria in general [10, 13].

The uPA-plg concept of proteolytic ENaC activation has been embraced as an attractive explanation for sodium retention in NS, as discussed in numerous reviews [6, 14-16] and even adopted in textbooks [17, 18]. However, the detection of plasmin in the urine together with its ability to activate ENaC *in vitro* is not sufficient to infer an essential role of urinary plasmin in ENaC-mediated sodium retention in NS *in vivo*. More direct evidence could be provided by a plg knockout model [19]. In two recent studies, our group followed the approach of utilizing knockout mouse models to define the *in vivo* role of the serine proteases plasma kallikrein (*klkb1*$^{-/-}$) [20] and urokinase-type plasminogen activator (*uPA*$^{-/-}$) [9] in ENaC-mediated sodium retention in experimental NS. Both serine proteases were found to stimulate ENaC currents *in vitro*, however, the lack of either one did not protect nephrotic mice from ENaC-mediated sodium retention. The results in nephrotic *uPA*$^{-/-}$ mice was the first evidence arguing against plasmin as the essential serine protease mediating sodium retention in NS as they excreted plg almost exclusively as zymogen. However, generation of trace amounts of plasmin by other serine proteases present in nephrotic urine of *uPA*$^{-/-}$ mice could not be excluded [9, 21].

In this study, we investigated the effect of plasminogen deficiency in a genetic model of experimental NS by generating double knockout mice (*nphs2*$^{\Delta ipod}$**plg*$^{-/-}$) lacking plasminogen and harboring an inducible podocyte-specific podocin (Nphs2) knockout. We observed that plg-deficient nephrotic mice were not protected from ENaC-mediated sodium retention, whereas treatment with the serine protease inhibitor aprotinin prevented sodium retention.

Results

A tet-on system driven by the nephrin (Nphs1) promoter leads to an efficient depletion of podocin (Nphs2) expression

We used a tetracycline-controlled transcriptional activation of a Cre recombinase (tet-on) under a podocyte-specific nephrin-driven promoter (Figure 1A) yielding a complete depletion of podocin expression at the protein level 14 days after end of induction (Figure 1B). In kidney samples from these *nphs2*$^{\Delta ipod}$ mice taken 14 days after end of induction, glomerular podocin expression was lost as analyzed by immunofluorescence microscopy (Figure 1C). This was accompanied by a loss of nephrin expression. On light microscopy, protein droplets were visible in dilated tubuli reflecting nephrotic-range proteinuria (Figure 1D). In the same samples, electron microscopy revealed foot process effacement (Figure 1E).

Plasminogen deficient mice have normal kidney structure and sodium handling

Nphs2$^{\Delta ipod}$ mice were intercrossed with constitutively plasminogen deficient mice (Bl6-Plg^{tm1Jld} or *plg*$^{-/-}$) to generate double knockout mice (*nphs2*$^{\Delta ipod}$**plg*$^{-/-}$). Compared to their littermates (*nphs2*$^{\Delta ipod}$**plg*$^{+/+}$), *nphs2*$^{\Delta ipod}$**plg*$^{-/-}$ mice had a reduced body weight (Supplemental Figure 2A) as a result of plasminogen deficiency which has been described in *plg*$^{-/-}$ mice previously and is related to damage of the liver and other organs such as the lung or gastrointestinal tract due to fibrin deposition [22]. In contrast, kidneys were spared from fibrin deposition in *plg*$^{-/-}$ and *nphs2*$^{\Delta ipod}$**plg*$^{-/-}$ mice ([22], Supplemental Figure 2B). Kidney function was not impaired in *nphs2*$^{\Delta ipod}$**plg*$^{-/-}$ mice as indicated by normal plasma urea and creatinine concentrations (Supplemental Figure 2C-D). In addition, urinary albumin excretion was not increased (Supplemental Figure 2E). Urinary sodium excretion and plasma aldosterone concentrations were not different in *nphs2*$^{\Delta ipod}$**plg*$^{-/-}$ under both a normal and a low salt diet excluding abnormal sodium handling (Table 1, Supplemental Figure 2F-G).

Nphs2$^{\Delta ipod}$**plg*$^{-/-}$ *mice develop nephrotic proteinuria devoid of urinary plasminogen excretion*

After the end of induction, *nphs2*$^{\Delta ipod}$**plg*$^{+/+}$ and *nphs2*$^{\Delta ipod}$**plg*$^{-/-}$ mice developed nephrotic proteinuria of a similar extent that was accompanied by similar hypoalbuminemia after 14 days (Figure 2A-B). In addition, there was a similar increase in the plasma concentration of cholesterol and a decrease in renal function, as evidenced by an increase in plasma urea and a tendency towards increased plasma creatinine concentration in nephrotic mice of both genotypes (Figure

2C-E). Plasma concentrations of aldosterone were not different in uninduced *nphs2$^{\Delta ipod}$*plg$^{+/+}$* and *nphs2$^{\Delta ipod}$*plg$^{-/-}$* mice and increased slightly after induction of nephrotic syndrome in both genotypes reaching statistical significance in nephrotic *nphs2$^{\Delta ipod}$*plg$^{-/-}$* mice (Figure 2F). In a Western blot from plasma and urine samples of uninduced and nephrotic mice (Figure 2G), albumin (69 kDa) and plasminogen (105 kDa) were not detectable in uninduced urine of *nphs2$^{\Delta ipod}$*plg$^{+/+}$* mice. In contrast, nephrotic urine contained albumin, plasminogen and also the heavy chain of plasminogen (80 kDa) indicating proteolytic activation by urokinase as published previously [9]. Nephrotic urine of *nphs2$^{\Delta ipod}$*plg$^{-/-}$* mice contained albumin, whereas plasminogen was absent in plasma and urine samples. Quantification of plasmin(ogen) excretion in the urine of *nphs2$^{\Delta ipod}$*plg$^{+/+}$* mice using ELISA showed a massive increase by more than three orders of magnitude within days, without affecting plasma concentration (Figure 2H). Using the chromogenic tripeptide substrate S-2251 (Val-Leu-Lys or VLK coupled the chromophore p-nitroaniline), urinary activity to liberate p-nitroaniline (so-called amidolytic activity) paralleled the increase in urinary plasmin(ogen) excretion and reflected active plasmin (Figure 2I). Notably, amidolytic activity was greatly reduced in *nphs2$^{\Delta ipod}$*plg$^{-/-}$* mice which can be explained by a dominant contribution of urinary plasmin to the amidolytic activity against the substrate used.

*Nephrotic nphs2$^{\Delta ipod}$*plg$^{+/+}$ and nphs2$^{\Delta ipod}$*plg$^{-/-}$ mice experience ENaC activation and sodium retention*

The natriuretic response to amiloride (10 µg g bw^{-1} i.p.) was determined to assess ENaC activity in uninduced and nephrotic *nphs2$^{\Delta ipod}$*plg$^{+/+}$* and *nphs2$^{\Delta ipod}$*plg$^{-/-}$* mice. Baseline natriuresis was determined from injection of vehicle (injectable water, 5 µl g bw^{-1}). As shown in Figure 3A, this response was similar in *nphs2$^{\Delta ipod}$*plg$^{+/+}$* and *nphs2$^{\Delta ipod}$*plg$^{-/-}$* before induction of nephrotic syndrome, indicating similar ENaC function in both genotypes. After induction of nephrotic syndrome, natriuretic response increased significantly in both genotypes reaching similar values. ENaC activation in nephrotic mice was most evident when the ratio of natriuresis between vehicle and amiloride was calculated, showing a significant increase in both genotypes (Figure 3B).

As a consequence, daily urinary sodium concentration dropped to minimal values of 6±1 mM (10±2 µmol mg $^{-1}$ crea) and 5±1 mM (7±2 µmol mg^{-1} crea) in *nphs2$^{\Delta ipod}$*plg$^{+/+}$* and *nphs2$^{\Delta ipod}$*plg$^{-/-}$* mice, respectively, during the course of experimental nephrotic syndrome despite constant food and fluid or sodium intake (Figure 3C, Supplemental Figure 3A-B, Table 1). The

positive sodium balance was also evident from studies of nephrotic mice in metabolic cages (Table 1). Subsequently, nephrotic mice of both genotypes gained body weight and developed ascites indicating sodium retention, while control mice did not. (Figure 3D, Supplemental Figure 3C). The maximal body weight gain was 21 ± 1% and 17 ± 2% in *nphs2*$^{\Delta ipod}$***plg*$^{+/+}$ and *nphs2*$^{\Delta ipod}$***plg*$^{-/-}$ mice, respectively, which was not significantly different (p=0.2192, Supplemental Figure 3D). Calculation of the area under the curve (AUC) of the body weight difference in each mouse showed no significant difference (p=0.6951, Supplemental Figure 3E). Chronologically, proteinuria was first observed as the sign of nephrotic syndrome in both *nphs2*$^{\Delta ipod}$***plg*$^{+/+}$ and *nphs2*$^{\Delta ipod}$***plg*$^{-/-}$ mice (Suppl. Fig. 3F, G). The increase of urinary amidolytic activity was in parallel with the development of proteinuria in *nphs2*$^{\Delta ipod}$***plg*$^{+/+}$ mice and was followed by a drop in the urinary sodium excretion. Subsequently, with a lag-time of one to two days, body weight increased in both genotypes. Unexpectedly, urinary sodium excretion increased spontaneously after day 9-10 in both genotypes, which was followed by complete remission of sodium retention (Figure 3C-D). This finding has also previously been described in doxorubicin-induced nephrotic syndrome in mice [23] and the PAN nephrosis model in rats [24].

Table 2 depicts the alterations of the plasma concentrations of electrolytes, hematocrit, and hemoglobin concentration as determined using a blood gas analyzer. Except for a slightly higher ionized Ca^{2+}, no differences in any parameter were noted in uninduced *nphs2*$^{\Delta ipod}$***plg*$^{+/+}$ and *nphs2*$^{\Delta ipod}$***plg*$^{-/-}$ mice. In the nephrotic state, plasma potassium concentrations were significantly increased compared to baseline in both genotypes. This has been analogously shown in nephrotic rats [25]. In nephrotic *nphs2*$^{\Delta ipod}$***plg*$^{-/-}$ mice, mild hypernatremia was present (Table 2).

Aprotinin prevents sodium retention in nephrotic nphs2$^{\Delta ipod}$***plg*$^{+/+}$ *and nphs2*$^{\Delta ipod}$***plg*$^{-/-}$ *mice*

In doxorubicin-induced murine nephrotic syndrome, sodium retention and ascites formation were completely prevented by the serine protease inhibitor aprotinin underscoring the essential role of serine proteases and proteolytic ENaC activation [4]. To reproduce this finding in nephrotic *nphs2*$^{\Delta ipod}$***plg*$^{+/+}$ mice and to analyze if excretion of serine proteases or proteasuria also accounted for the sodium retention in *nphs2*$^{\Delta ipod}$***plg*$^{-/-}$ mice, we implanted sustained-release pellets containing aprotinin (2 mg per day) or placebo pellets subcutaneously on day 3 (after end of induction) in both genotypes. Urinary aprotinin concentrations reached maximal values between 667 – 773 µg ml^{-1} in both genotypes while the plasma concentration was two orders of magnitude lower 5 days after pellets implantation (Figure 4A). Aprotinin had no impact on proteinuria

quantitatively, however suppressed its amidolytic activity completely in nephrotic *nphs2$^{\Delta ipod}$*plg$^{+/+}$* and *nphs2$^{\Delta ipod}$*plg$^{-/-}$* mice (Figure 4B-C). Urinary sodium excretion dropped in placebo-treated nephrotic *nphs2$^{\Delta ipod}$*plg$^{+/+}$* and *nphs2$^{\Delta ipod}$*plg$^{-/-}$* mice, while aprotinin-treated nephrotic mice of both genotypes remained constant, indicating suppression of proteolytic ENaC activation (Figure 4D). This led to prevention of body weight gain and ascites formation in aprotinin-treated nephrotic *nphs2$^{\Delta ipod}$*plg$^{+/+}$* and *nphs2$^{\Delta ipod}$*plg$^{-/-}$* mice while placebo-treated nephrotic mice of both genotypes gained body weight and developed ascites (Figure 4E). Under aprotinin treatment, plasma aldosterone tended to be reduced compared to placebo treated mice (Figure 4F).

*Expression of ENaC subunits in kidney tissues from nephrotic nphs2$^{\Delta ipod}$*plg$^{+/+}$ and nphs2$^{\Delta ipod}$*plg$^{-/-}$ mice*

Histological analyses of formalin-fixed kidney tissues revealed up-regulation and apical targeting of α- and γ-ENaC staining in nephrotic *nphs2$^{\Delta ipod}$*plg$^{+/+}$ and nphs2$^{\Delta ipod}$*plg$^{-/-}$* mice which was similar under aprotinin treatment (Figure 5). Western blot analyses from membrane protein fractions of kidney cortex for α-ENaC revealed two specific bands for α-ENaC at 87 and 26 kDa and two bands for γ-ENaC at 84 and 72 kDa all of which disappeared after application of the immunogenic peptide (Suppl. Fig. 4). The largest bands at 87 kDa and 84 kDa most likely represent full-length α-ENaC and γ-ENaC, respectively, whereas the band at 26 kDa represents the furin cleavage product of α-ENaC and that at 72 kDa furin-cleaved γ-ENaC. For β-ENaC, there was only a single band at 85 kDa.

As shown in Fig. 6 and Table 3, expression of the α- and β-ENaC subunits were not significantly altered in nephrotic *nphs2$^{\Delta ipod}$*plg$^{+/+}$* and *nphs2$^{\Delta ipod}$*plg$^{-/-}$* mice except for a tendency towards increased expression of the 26 kDa α-ENaC fragment. Expression of full-length γ-ENaC (84 kDa) was not different in all conditions and genotypes. However, expression of furin-cleaved γ-ENaC (72 kDa) increased in nephrotic *nphs2$^{\Delta ipod}$*plg$^{+/+}$* mice which was normalized by aprotinin treatment (Table 3). In *nphs2$^{\Delta ipod}$*plg$^{-/-}$* mice, the tendency of the changes was similar, however, the variability precluded significant differences.

As in previous efforts, we could not detect a specific band corresponding to fully-cleaved γ-ENaC between 65 to 67 kDa in renal cortex tissue from uninduced wild-type or nephrotic mice (Fig. 6, Suppl. Fig. 4).

Discussion

Our study demonstrates that mice with an inducible podocin deletion driven by the nephrin promoter (*nphs2*$^{\Delta ipod}$) develop all features of NS, including massive proteinuria, hypoalbuminemia, hyperlipidemia, and most importantly sodium retention. The model was strikingly similar to the doxorubicin-induced NS model developed by our group [23, 26, 27]. A characteristic feature of both nephrotic models is the high proteinuria, which exceeds a threshold of 100 – 140 mg protein mg^{-1} creatinine (corresponding to > 50 – 70 mg protein 24 h^{-1}) that seems to be a prerequisite for the development of sodium retention [4, 23]. This relates to the high efficiency of nephrin driven expression of Cre recombinase and podocin deletion in the model used, which was at least as efficient if not superior to tamoxifen-driven podocin deletion [28, 29]. Of note, podocin deletion was accompanied by a disappearance of nephrin expression, indicating a breakdown of the slit diaphragm and possibly explaining the high level of proteinuria.

The development of sodium retention in this model allows for investigating its underlying mechanisms. As with doxorubicin-induced nephrotic syndrome, the current model contains elements of both the overfill and underfill theories, which are not mutually exclusive [3, 26]. The data are consistent with a key role of the urinary excretion of active serine proteases or proteasuria that activate ENaC by endoluminal proteolysis. This would be in agreement with the overfill hypothesis. In addition, activation of the renin angiotensin aldosterone system might indicate arterial underfill and aggravate sodium retention by upregulation of membrane expression of furin-cleaved ENaC. However, aldosterone secretion might vary according to the severity of the underlying underfill and therefore explains the large scatter of the plasma aldosterone concentration found in the mice, which reached a significant increase in *nphs2*$^{\Delta ipod}$**plg*$^{-/-}$ mice. The inhibitory effect of aprotinin on aldosterone secretion has been observed in doxorubicin-induced nephrotic syndrome as well and remains unclear [4].

Plasmin has been proposed as the key serine protease to mediate renal sodium retention in NS [5, 6, 12]. This interpretation was related to the high abundance of plasmin in nephrotic urine and the ability to stimulate ENaC currents *in vitro* by cleavage of human γ-ENaC, which may take place at two distinct sites (K189 and RKRK178) [10, 11]. However, a definitive experimental proof from a genetic mouse model lacking plasminogen was pending [19]. In this study we confirm that urine from nephrotic *nphs2*$^{\Delta ipod}$ mice also contained large amounts of plasminogen and active plasmin as previously shown to be the case in mice with doxorubicin-induced nephrotic syndrome [4]. By

generating *nphs2*$^{\Delta ipod}$**plg*$^{-/-}$ mice, we were able to provide further evidence on the role of plasminogen in ENaC-mediated sodium retention in experimental NS. Our results clearly demonstrate that plasminogen deficiency does not protect from ENaC activation and sodium retention. However, aprotinin treatment was still effective in nephrotic *nphs2*$^{\Delta ipod}$**plg*$^{-/-}$ mice, underscoring the essential role of other serine proteases in the absence of plasmin (Figure 7). The activity of these proteases was suggested by the residual amidolytic activity *nphs2*$^{\Delta ipod}$**plg*$^{-/-}$ mice, as shown in Fig. 2F.

The result of the present study is in good agreement with the results obtained in nephrotic *uPA*$^{-/-}$ mice, which developed similar ENaC activation and sodium retention as wild-type mice despite an almost complete absence of plasminogen conversion to plasmin [9]. Similar findings were reported in podocin deficient nephrotic mice treated with an antibody inhibiting tubular uPA activity [29]. In both studies, trace amounts of plasmin could not be ruled out. Controversy arose about the interpretation of sodium retention in both studies [21, 30, 31]. Whereas both studies demonstrated identical body weight gain and ascites formation in nephrotic uPA-deficient and uPA-inhibited mice until day 14, there was a positive sodium balance of uPA inhibited mice at day 18 [29]. This let the authors conclude that uPA-plg contributes, but not solely explains sodium retention. However, the evidence from sodium balance data derived from metabolic cages must be interpreted with caution because it is highly error-prone due to occult urine losses [32]. For a meaningful interpretation, data on sodium balance should be paralleled by corresponding changes in body weight as 1 g of body weight gain is equal to 150 µmol of retained Na^+. In the present study, sodium-replete uninduced mice had seemingly positive sodium balance despite constant weight and euvolemia pointing to occult urinary losses (Table 1). Hence, our approach to quantify sodium retention in mouse models relies on the combination of body weight gain, development of ascites, and reduced urinary sodium excretion in spot urine sample despite normal food intake. The determination of sodium balance or quantitation of ascites is omitted to the high error.

The lack of an effect of uPA and plg deletion on sodium retention strongly argues against the current concept of uPA/plasmin-mediated proteolytic ENaC activation in NS. We are convinced that this insight will stimulate further efforts to identify those aprotinin-sensitive serine proteases that are excreted in NS and could mediate proteolytic ENaC activation (Figure 7). It should be underscored that any candidate serine protease should be tested in a model of experimental nephrotic syndrome *in vivo* with abrupt body weight gain as gold standard to indicate sodium

retention. However, it is conceivable that redundant serine proteases might act in cascades to mediate proteolytic ENaC activation in experimental nephrotic syndrome which might not be elucidated using single knockout models. With this regard, aprotinin´s effect could also rely on the inhibition of multiple serine proteases that might participate in proteolytic ENaC activation.

Expression analyses of ENaC subunits using immunohistochemistry demonstrated upregulation of α- and γ-ENaC at the apical membrane. This finding is referred to as apical targeting and corresponds to increased expression of furin-cleaved α- and γ-ENaC, the dominant form of ENaC found in the plasma membrane [33]. This corresponded to increased expression of furin-cleaved α- and γ-ENaC in Western blot and most likely reflects the impact of increased aldosterone secretion. However, detection of fully cleaved γ-ENaC was elusive in this (C57Bl6 mice) and all other studies with murine experimental NS (129/SvImJ mice), at least by our group, and remains an unmet experimental challenge. In the samples from nephrotic mice the proportion of fully cleaved ENaC protein localized in the apical membrane was probably below the detection limit of our Western blot analysis. Thus, at present we cannot provide definitive evidence to show that in NS filtered urinary serine proteases increase the proportion of fully cleaved γ-ENaC at the cell surface of renal tubular cells. Along the lines, it should be remembered that ENaC regulation is known to be highly complex [34, 35]. In addition to proteases other extracellular and intracellular factors such as Na^+ concentration, regulatory proteins, phosphorylation status, acidic phospholipids or palmitoylation may modulate ENaC function in NS.

In conclusion, we demonstrate that plg deficient nephrotic mice were not protected from ENaC-mediated sodium retention, whereas treatment with the serine protease inhibitor aprotinin prevented sodium retention. The latter finding underscores the essential role of other serine proteases in mediating sodium retention in NS in the absence of plasminogen.

Methods

*Generation of nphs2$^{\Delta ipod}$*plg$^{-/-}$ mice*

Mice with two floxed podocin alleles were mated with mice harboring transgenes for a tetracycline-controlled transcriptional activation of a Cre recombinase under a podocyte-specific nephrin-driven promoter (Bl6-Nphs2$^{tm3.1Antc}$*Tg(Nphs1-rtTA*3G)^{8Jhm}*Tg(tetO-cre)^{1Jaw} or *nphs2$^{\Delta ipod}$*). These mice were a kind gift from Géraldine Mollet and Corinne Antignac (Imagine Institute of Genetic Diseases, Paris, France, first published in 2009 [36]) and intercrossed with plasminogen deficient mice (Bl6-Plg^{tm1Jld} or *plg$^{-/-}$,* [22]) to yield double knockout mice (*nphs2$^{\Delta ipod}$*plg$^{-/-}$*) and littermates (*nphs2$^{\Delta ipod}$*plg$^{+/+}$*). All mice were on a pure C57Bl/6 background and all genotypes were born at the expected Mendelian frequency. Genotyping was performed using PCR with the conditions and primers shown in Suppl. Table 1&2. Mice with two floxed podocin alleles lacking the Cre recombinase or the podocyte-specific nephrin-driven promoter were used as control mice.

Mouse studies

Experiments were performed on 3-month-old *nphs2$^{\Delta ipod}$*plg$^{-/-}$* and *nphs2$^{\Delta ipod}$*plg$^{+/+}$* littermate mice of both sexes. Mice were kept on a 12:12-h light-dark cycle and fed a standard diet (ssniff, sodium content 0.24% corresponding to 104 µmol g^{-1}, Soest, Germany) with tap water ad libitum. Deletion of the podocin alleles leading to experimental nephrotic syndrome was induced after a 14-day treatment with doxycycline in the drinking water (2 g L^{-1} with 5% sucrose) and the end of induction treatment was designated as day 0. Different sets of mice for used to study sodium handling, amiloride-sensitive natriuresis, the course of nephrotic syndrome and the effect of the serine protease inhibitor aprotinin (Suppl. Fig. 1). In uninduced *nphs2$^{\Delta ipod}$*plg$^{-/-}$* and *nphs2$^{\Delta ipod}$*plg$^{+/+}$* mice, sodium balance was studied in metabolic cages for 2 days of a control diet (C1000, Altromin, Lage, Germany, sodium content 106 µmol g^{-1}) followed by 5 days on a low salt diet (C1036, Altromin, Lage, Germany, sodium content 7 µmol g^{-1} food, Suppl. Fig. 1A). To assess ENaC activity, amiloride-natriuresis was studied before and during avid sodium retention on day 7 and day 8 after end of induction. To this end, mice were injected with vehicle (5 µl $^{-1}$g body weight [bw] injectable water, day 7) and amiloride (10 µg g $^{-1}$ bw) on the other day (day 8) to determine urinary sodium excretion during 6 h after injection (Suppl. Fig. 1A). Amiloride-sensitive natriuresis was expressed as ratio of from both values. Due to restrictions by the regulating authority and the IACUC which would not allow to study mice in metabolic cages for

sodium balance over 14 days, we kept single mice in normal cages and collected spontaneously voided urine in the morning between 8 and 9 a.m. up to 14 days. Daily body weight, food and fluid intake were monitored by weighing the food pellets and the water bottles (Suppl. Fig. 1B). Blood samples were drawn before induction and at sacrifice on day 14. Treatment with the serine protease inhibitor aprotinin was performed using custom-made subcutaneous pellets with a matrix-driven sustained release (Innovative Research of America, Florida, USA). Aprotinin-containing or placebo pellets consisting of the matrix only were surgically implanted subcutaneously on the back of the mice on day 3 after end of induction (Suppl. Fig. 1C). The optimal dose chosen after dose-finding studies was 2 mg per day for bovine aprotinin (6000 KIU mg^{-1}, Loxo, Heidelberg, Germany). Blood samples and kidneys were collected at sacrifice on day 8. All animal experiments were conducted according to the National Institutes of Health Guide for the Care and Use of Laboratory Animals and the German law for the welfare of animals, and they were approved by local authorities (Regierungspraesidium Tuebingen, approval number M 15/17).

Laboratory measurements

Urinary activity of plasmin was measured using the chromogenic substrate S-2251 (Haemochrom, Essen, Germany). 3 µL urine and 50 µL 2 mM substrate was incubated for 1 h at 37°C with or without aprotinin (final concentration 20 µg mL^{-1}). Absorption was analyzed at 405 nm on a 96-well plate reader (Biotek EL800, VT, USA). The difference between the optical density with or without aprotinin reflected the specific activity of plasmin. Values were expressed as relative units (1000*Delta absorption @405 nm) and normalized to urinary creatinine concentration.

Urinary creatinine was measured with a colorimetric Jaffé assay, plasma creatinine, cholesterol and urea with enzymatic assays (Labor+Technik, Berlin, Germany), urinary protein concentration using the Bradford method (Bio-Rad Laboratories, Munich, Germany) and urinary and fecal sodium concentration with flame photometry (Eppendorf EFUX 5057, Hamburg, Germany). Feces was dried, weighed and dissolved in 1 M HNO_3. Both urinary protein and sodium concentration were normalized to the urinary creatinine concentration. Plasma aldosterone was measured using an ELISA kit (IBL, Hamburg, Germany), plasma albumin using a fluorometric kit against mouse albumin as standard (Active motif, Carlsbad, USA). Urinary and plasma plasminogen concentration were measured using an ELISA kit (Loxo, Heidelberg, Germany) that detects both plasmin and plasminogen was designated by plasmin(ogen). Urinary aprotinin concentration was determined using an ELISA kit (Cloud-clone corp, China). Venous blood gas analysis was done

using an IL GEM® Premier 3000 blood gas analyzer (Instrumentation Laboratory, Munich, Germany).

Western blot from urine samples and kidney tissue of mice

For Western blot (WB) analysis of albumin and plasminogen excretion in the urine of nephrotic mice, SDS-PAGE on an 8% gel was performed with 10 µg urinary protein per lane (or maximal volume when protein <10µg). WB analysis of α-, β-, and γ-ENaC expression from renal tissue was performed as previously described [4, 9]. Proteins of interest were detected with secondary antibodies labelled with fluorescent infrared dyes on a fluorescence scanner (Licor Odyssey, Lincoln, USA). For loading control, total protein was measured using Revert Total Protein Stain (Licor, Lincoln, USA). WB for podocin expression was done from isolated glomeruli as described previously [37].

Primary Antibodies

Antibodies against murine α-, β-, and γ-ENaC were raised in rabbits against the amino acids 45-68 for α-ENaC, 617-638 for β-ENaC and 634–655 for γ-ENaC (Pineda, Berlin, Germany) [38, 39]. Antisera containing antibodies against α- and γ-ENaC were purified with affinity chromatography. In addition, γ-ENaC was probed in Western blot with a commercially available antibody directed against the same immunogenic peptide (SPC-405, Stressmarq). To confirm that the observed bands were specific for α- and γ-ENaC, the primary antibodies were preincubated with each immunogenic peptide (20x excess by molarity) overnight at 4 °C. Plasminogen was probed using a rabbit antibody directed against amino acid residues 84-434 of the heavy chain (ab154560, abcam). This antibody detects plasminogen zymogen at 105 kDa and plasminogen heavy chain at 80 kDa after cleavage and dissociation from the light chain under reducing WB conditions. Albumin and nephrin were detected using antibodies from R&D systems (AF3329 and AF3159), podocin using an antibody from Sigma (P0372).

Immunohistochemistry and immunofluorescence from kidney tissue

Paraffin-embedded formalin-fixed sections (2µm) were deparaffinized and rehydrated using standard protocols. Kidney sections were blocked for 15 minutes with normal goat serum diluted 1:5 in 50 mM tris(hydroxymethyl)-aminomethane(Tris), pH 7.4, supplemented with 1% (w/v) skim milk (Bio-Rad Laboratories, Munich, Germany), followed by incubation with previously mentioned primary antibodies (rabbit anti-γ-ENaC, 1:50 or rabbit anti-α-ENaC, 1:1000) for 1

hour, at 37 °C, and subsequent washing in Tris buffer (50 mM Tris, pH 7.4, supplemented with 0.05% (v/v) Tween 20 (Sigma-Aldrich, Munich, Germany; 3 x 5 minutes). The secondary antibody (a biotinylated goat anti-rabbit, Vector Laboratories, Burlingame, CA USA; 1:500) was applied for 30 minutes. Sections were further processed using the VectaStain ABC kit according to the manufacturer's instructions and DABImmpact (both Vector Laboratories) as substrate. Finally, the sections were counterstained in hemalaun, dehydrated, and mounted for observation using an Olympus Bx60 upright microscope.

For immunofluorescence, formalin-fixed sections were deparaffinized, rehydrated and subsequently stained for podocin, nephrin and nuclei as described previously [40].

Electronmicroscopy

For electron microscopy a small piece of mouse renal cortex was immersion fixed in 4% PFA and 1% (v/v) glutaraldehyde in 0.1M PB. After post-fixation (same fixative o/n at 4°C), tissue blocks were washed in 0.1 M PB, treated with OsO_4 (0.5% for 60 min) and stained with uranyl acetate (1% w/v in 70% v/v Ethanol). After dehydration tissue blocks were embedded in epoxy resin (Durcupan ACM, Sigma-Aldrich, Gillingham, UK). 40nm ultrathin sections were cut on an UC6 ultramicrotome (Leica, Wetzlar, Germany) and analysed using an 80kV Philipps CM100 transmission electron microscope and Olympus ITEM software.

Statistical analysis

Data are provided as means with SEM. Data were tested for normality with the Kolmogorov-Smirnov-Test, D'Agostino and Pearson omnibus normality test and Shapiro-Wilk-Test. Variances were tested using the Bartlett´s test for equal variances. Data from repeated measurements were tested for significance using one-way ANOVA, and data from two groups were tested with paired or unpaired Student's t-test, Mann-Whitney U-test using GraphPad Prism 8, GraphPad Software (San Diego, CA, www.graphpad.com). Densitometric analysis of western blots was done using Image Studio Version 3.1.4 (Licor). A p value <0.05 by two-tailed testing was considered statistically significant.

Acknowledgments

The artwork in Figure 7 by Marina Corral Spence and Hao Tian is acknowledged.

Disclosures.

None.

Author contributions

MX, BNB, HA, OK, FG, MW, UA, MW, AJ, DE, CD data acquisition and analysis, editing of the manuscript; KA, TBH, EFP, ALB discussion of the results, editing of the manuscript;
FA conceived and designed the work, data interpretation, drafting of the manuscript

Funding

These studies were supported by grant from the German Research foundation (AR 1092/2-1) to FA and SFB KIDGEM Project A01 and A03 to FG and TBH. TBH was supported by the DFG (CRC 1192, HU 1016/8-2), by the BMBF (STOP-FSGS01GM1901C) and by the European Research Council (ERC grant 61689, DNCure). EFP was supported by a grant from the NIH (2 P01 HL076491).

References

1. Kleyman, TR, Carattino, MD, Hughey, RP: ENaC at the cutting edge: regulation of epithelial sodium channels by proteases. *J Biol Chem,* 284**:** 20447–20451, 2009.
2. Ray, EC, Rondon-Berrios, H, Boyd, CR, Kleyman, TR: Sodium retention and volume expansion in nephrotic syndrome: implications for hypertension. *Adv Chronic Kidney Dis,* 22**:** 179-184, 2015.
3. Artunc, F, Worn, M, Schork, A, Bohnert, BN: Proteasuria-The impact of active urinary proteases on sodium retention in nephrotic syndrome. *Acta physiologica (Oxford, England),* 225**:** e13249, 2019.
4. Bohnert, BN, Menacher, M, Janessa, A, Worn, M, Schork, A, Daiminger, S, Kalbacher, H, Haring, HU, Daniel, C, Amann, K, Sure, F, Bertog, M, Haerteis, S, Korbmacher, C, Artunc, F: Aprotinin prevents proteolytic epithelial sodium channel (ENaC) activation and volume retention in nephrotic syndrome. *Kidney international,* 93**:** 159-172, 2018.
5. Svenningsen, P, Bistrup, C, Friis, UG, Bertog, M, Haerteis, S, Krueger, B, Stubbe, J, Jensen, ON, Thiesson, HC, Uhrenholt, TR, Jespersen, B, Jensen, BL, Korbmacher, C, Skøtt, O: Plasmin in nephrotic urine activates the epithelial sodium channel. *J Am Soc Nephrol,* 20**:** 299–310, 2009.
6. Passero, CJ, Hughey, RP, Kleyman, TR: New role for plasmin in sodium homeostasis. *Curr Opin Nephrol Hypertens,* 19**:** 13-19, 2010.
7. Staehr, M, Buhl, KB, Andersen, RF, Svenningsen, P, Nielsen, F, Hinrichs, GR, Bistrup, C, Jensen, BL: Aberrant glomerular filtration of urokinase-type plasminogen activator in nephrotic syndrome leads to amiloride-sensitive plasminogen activation in urine. *Am J Physiol Renal Physiol,* 309**:** F235-241, 2015.
8. Wagner, SN, Atkinson, MJ, Wagner, C, Hofler, H, Schmitt, M, Wilhelm, O: Sites of urokinase-type plasminogen activator expression and distribution of its receptor in the normal human kidney. *Histochemistry and cell biology,* 105**:** 53-60, 1996.
9. Bohnert, BN, Daiminger, S, Worn, M, Sure, F, Staudner, T, Ilyaskin, AV, Batbouta, F, Janessa, A, Schneider, JC, Essigke, D, Kanse, S, Haerteis, S, Korbmacher, C, Artunc, F: Urokinase-type plasminogen activator (uPA) is not essential for epithelial sodium channel (ENaC)-mediated sodium retention in experimental nephrotic syndrome. *Acta physiologica (Oxford, England)***:** e13286, 2019.
10. Schork, A, Woern, M, Kalbacher, H, Voelter, W, Nacken, R, Bertog, M, Haerteis, S, Korbmacher, C, Heyne, N, Peter, A, Haring, HU, Artunc, F: Association of Plasminuria with Overhydration in Patients with CKD. *Clinical journal of the American Society of Nephrology : CJASN,* 11**:** 761-769, 2016.

11. Haerteis, S, Krappitz, M, Diakov, A, Krappitz, A, Rauh, R, Korbmacher, C: Plasmin and chymotrypsin have distinct preferences for channel activating cleavage sites in the gamma subunit of the human epithelial sodium channel. *The Journal of general physiology,* 140**:** 375–389, 2012.
12. Passero, CJ, Mueller, GM, Rondon-Berrios, H, Tofovic, SP, Hughey, RP, Kleyman, TR: Plasmin activates epithelial Na+ channels by cleaving the gamma subunit. *J Biol Chem,* 283**:** 36586–36591, 2008.
13. Ray, E, Miller, R, JE, D, T, C, Kinlough, C, CL, D, Unruh, M, Orchard, T, Kleyman, T: Urinary Plasmin(ogen) as a Prognostic Factor for Hypertension. *Kidney international reports,* 3**:** 1434–1442, 2018.
14. Svenningsen, P, Friis, UG, Versland, JB, Buhl, KB, Moller Frederiksen, B, Andersen, H, Zachar, RM, Bistrup, C, Skott, O, Jorgensen, JS, Andersen, RF, Jensen, BL: Mechanisms of renal NaCl retention in proteinuric disease. *Acta physiologica (Oxford, England),* 207**:** 536-545, 2013.
15. Siddall, EC, Radhakrishnan, J: The pathophysiology of edema formation in the nephrotic syndrome. *Kidney international,* 82**:** 635-642, 2012.
16. Svenningsen, P, Andersen, H, Nielsen, LH, Jensen, BL: Urinary serine proteases and activation of ENaC in kidney--implications for physiological renal salt handling and hypertensive disorders with albuminuria. *Pflügers Archiv : European journal of physiology,* 467**:** 531–542, 2015.
17. Skorecki, K, Chertow, GM, Marsden, PA, Taal, MW, Yu, ASL: Brenner and Rector's The Kidney, 2-Volume Set, 10th Edition. In, 2016, pp 2800.
18. Swiatecka-Urban, A, Woroniecki, RP, Kaskel, FJ: *Nephrotic Syndrome in Pediatric Patients*, 2017.
19. Kleyman, TR, Hughey, RP: Plasmin and Sodium Retention in Nephrotic Syndrome. *J Am Soc Nephrol,* 20**:** 233-234, 2009.
20. Haerteis, S, Schork, A, Dörffel, T, Bohnert, BN, Nacken, R, Wörn, M, Xiao, M, Essigke, D, Janessa, A, Schmaier, AH, Feener, EP, Haring, HU, Bertog, M, Korbmacher, C, Artunc, F: Plasma kallikrein activates the epithelial sodium channel (ENaC) in vitro but is not essential for volume retention in nephrotic mice. *Acta physiologica (Oxford, England),* 224(1)**:** e13060, 2018.
21. Ehmke, H: Sodium retention by uPA in nephrotic syndrome? *Acta physiologica (Oxford, England)***:** e13393, 2019.

22. Bugge, TH, Flick, MJ, Daugherty, CC, Degen, JL: Plasminogen deficiency causes severe thrombosis but is compatible with development and reproduction. *Genes & Development,* 9**:** 794-807, 1995.
23. Artunc, F, Nasir, O, Amann, K, Boini, KM, Haring, HU, Risler, T, Lang, F: Serum- and glucocorticoid-inducible kinase 1 in doxorubicin-induced nephrotic syndrome. *Am J Physiol Renal Physiol,* 295**:** F1624-1634, 2008.
24. Deschenes, G, Doucet, A: Collecting duct (Na+/K+)-ATPase activity is correlated with urinary sodium excretion in rat nephrotic syndromes. *J Am Soc Nephrol,* 11, 2000.
25. Ydegaard, R, Svenningsen, P, Bistrup, C, Andersen, RF, Stubbe, J, Buhl, KB, Marcussen, N, Hinrichs, GR, Iraqi, H, Zamani, R, Dimke, H, Jensen, BL: Nephrotic syndrome is associated with increased plasma K(+) concentration, intestinal K(+) losses and attenuated urinary K(+) excretion - studies in rats and humans. *Am J Physiol Renal Physiol*, 2019.
26. Bohnert, BN, Artunc, F: Induction of nephrotic syndrome in mice by retrobulbar injection of doxorubicin and prevention of volume retention by sustained release aprotinin. *Journal of Visualized Experiments,* 135**:** e57642, 2018.
27. Bohnert, BN, Dorffel, T, Daiminger, S, Calaminus, C, Aidone, S, Falkenau, A, Semrau, A, Le, MJ, Iglauer, F, Artunc, F: Retrobulbar Sinus Injection of Doxorubicin is More Efficient Than Lateral Tail Vein Injection at Inducing Experimental Nephrotic Syndrome in Mice: A Pilot Study. *Laboratory animals***:** 23677218824382, 2019.
28. Larionov, A, Dahlke, E, Kunke, M, Zanon Rodriguez, L, Schiessl, IM, Magnin, JL, Kern, U, Alli, AA, Mollet, G, Schilling, O, Castrop, H, Theilig, F: Cathepsin B increases ENaC activity leading to hypertension early in nephrotic syndrome. *Journal of cellular and molecular medicine*, 2019.
29. Hinrichs, GR, Weyer, K, Friis, UG, Svenningsen, P, Lund, IK, Nielsen, R, Mollet, G, Antignac, C, Bistrup, C, Jensen, BL, Birn, H: Urokinase-type plasminogen activator contributes to amiloride-sensitive sodium retention in nephrotic range glomerular proteinuria in mice. *Acta physiologica (Oxford, England)***:** e13362, 2019.
30. Bohnert, BN, Kanse, S, Haerteis, S, Korbmacher, C, Artunc, F: Rebuttal to editorial: Sodium retention by uPA in nephrotic syndrome? *Acta physiologica (Oxford, England)***:** e13427, 2019.
31. Hinrichs, GR, Weyer, K, Friis, UG, Svenningsen, P, Lund, IK, Nielsen, R, Mollet, G, Antignac, C, Bistrup, C, Jensen, BL, Birn, H: Sodium retention by uPA-plasmin-ENaC in nephrotic syndrome The authors reply. *Acta physiologica (Oxford, England)***:** e13432, 2019.

32. Nizar, JM, Bouby, N, Bankir, L, Bhalla, V: Improved protocols for the study of urinary electrolyte excretion and blood pressure in rodents: use of gel food and stepwise changes in diet composition. *American journal of physiology Renal physiology,* 314**:** F1129-F1137, 2018.
33. Frindt, G, Gravotta, D, Palmer, LG: Regulation of ENaC trafficking in rat kidney. *J Gen Physiol,* 147**:** 217-227, 2016.
34. Kleyman, TR, Kashlan, OB, Hughey, RP: Epithelial Na(+) Channel Regulation by Extracellular and Intracellular Factors. *Annu Rev Physiol,* 80**:** 263-281, 2018.
35. Kleyman, TR, Eaton, DC: Regulating ENaC's gate. *American journal of physiology Cell physiology*, 2019.
36. Mollet, G, Ratelade, J, Boyer, O, Muda, AO, Morisset, L, Lavin, TA, Kitzis, D, Dallman, MJ, Bugeon, L, Hubner, N: Podocin inactivation in mature kidneys causes focal segmental glomerulosclerosis and nephrotic syndrome. *J Am Soc Nephrol,* 20, 2009.
37. Boerries, M, Grahammer, F, Eiselein, S, Buck, M, Meyer, C, Goedel, M, Bechtel, W, Zschiedrich, S, Pfeifer, D, Laloe, D, Arrondel, C, Goncalves, S, Kruger, M, Harvey, SJ, Busch, H, Dengjel, J, Huber, TB: Molecular fingerprinting of the podocyte reveals novel gene and protein regulatory networks. *Kidney international,* 83**:** 1052-1064, 2013.
38. Nesterov, V, Krueger, B, Bertog, M, Dahlmann, A, Palmisano, R, Korbmacher, C: In Liddle Syndrome, Epithelial Sodium Channel Is Hyperactive Mainly in the Early Part of the Aldosterone-Sensitive Distal Nephron. *Hypertension,* 67**:** 1256-1262, 2016.
39. Krueger, B, Haerteis, S, Yang, L, Hartner, A, Rauh, R, Korbmacher, C, Diakov, A: Cholesterol depletion of the plasma membrane prevents activation of the epithelial sodium channel (ENaC) by SGK1. *Cell Physiol Biochem,* 24**:** 605-618, 2009.
40. Grahammer, F, Nesterov, V, Ahmed, A, Steinhardt, F, Sandner, L, Arnold, F, Cordts, T, Negrea, S, Bertog, M, Ruegg, MA, Hall, MN, Walz, G, Korbmacher, C, Artunc, F, Huber, TB: mTORC2 critically regulates renal potassium handling. *J Clin Invest,* 126**:** 1773-1782, 2016.
41. Lin, X, Suh, JH, Go, G, Miner, JH: Feasibility of repairing glomerular basement membrane defects in Alport syndrome. *J Am Soc Nephrol,* 25**:** 687-692, 2014.
42. Perl, AK, Wert, SE, Nagy, A, Lobe, CG, Whitsett, JA: Early restriction of peripheral and proximal cell lineages during formation of the lung. *Proceedings of the National Academy of Sciences of the United States of America,* 99**:** 10482-10487, 2002.
43. Suelves, M, Lopez-Alemany, R, Lluis, F, Aniorte, G, Serrano, E, Parra, M, Carmeliet, P, Munoz-Canoves, P: Plasmin activity is required for myogenesis in vitro and skeletal muscle regeneration in vivo. *Blood,* 99**:** 2835-2844, 2002.

Table 1: Sodium balance in *nphs2$^{\Delta ipod}$*plg$^{+/+}$* and *nphs2$^{\Delta ipod}$*plg$^{-/-}$* mice during various conditions

Values for uninduced mice under low salt diet were taken on the 5th day after initiating a low salt diet. Values for nephrotic mice were taken on day 8 of nephrotic syndrome.

Arithmetic means ± SEM (n= 8-11 each).

$^{\#}$ significant difference compared to uninduced mice of the same genotype under a control diet, * significant difference between genotypes

	uninduced control diet		uninduced low salt diet		nephrotic control diet	
	*nphs2$^{\Delta ipod}$*plg$^{+/+}$*	*nphs2$^{\Delta ipod}$*plg$^{-/-}$*	*nphs2$^{\Delta ipod}$*plg$^{+/+}$*	*nphs2$^{\Delta ipod}$*plg$^{-/-}$*	*nphs2$^{\Delta ipod}$*plg$^{+/+}$*	*nphs2$^{\Delta ipod}$*plg$^{-/-}$*
total Na^+ intake, µmol 24 h^{-1}	290 ± 14	322 ±16	23 ± 1 $^{\#}$	24 ± 1 $^{\#}$	258 ± 15	304 ± 13
urinary Na^+ excretion, µmol 24 h^{-1}	193 ± 16	229 ± 11 *	18 ± 3 $^{\#}$	16 ± 3 $^{\#}$	15 ± 6 $^{\#}$	25 ± 7 $^{\#}$
fecal Na^+ excretion, µmol 24 h^{-1}	13 ± 1	19 ± 3	7 ± 1	13 ± 2	11 ± 2	21 ± 2 *
Na^+ balance, µmol 24 h^{-1}	84 ± 13	74 ±14	-2 ± 3 $^{\#}$	-5 ± 3 $^{\#}$	232 ± 18 $^{\#}$	258 ± 15 $^{\#}$

Table 2: Plasma parameters obtained from venous blood gas analysis in *nphs2$^{\Delta ipod}$*plg$^{+/+}$* and *nphs2$^{\Delta ipod}$*plg$^{-/-}$* mice before and 14 days after induction of nephrotic syndrome.

Arithmetic means ± SEM (n=8-11 each)

[#] significant difference between uninduced and nephrotic mice of the same genotype, [*] significant difference between genotypes

Abbreviations: std standard, Hct haematocrit, cHb calculated haemoglobin concentration

	uninduced		nephrotic	
	*nphs2$^{\Delta ipod}$*plg$^{+/+}$*	*nphs2$^{\Delta ipod}$*plg$^{-/-}$*	*nphs2$^{\Delta ipod}$*plg$^{+/+}$*	*nphs2$^{\Delta ipod}$*plg$^{-/-}$*
venous pH	7.28 ± 0.02	7.24 ± 0.01	7.31 ± 0.01	7.23 ± 0.02 *
std HCO_3^-, mM	22 ± 0.9	21 ± 0.8	25 ± 0.6 #	22 ± 0.8
Na^+, mM	147 ± 0	150 ± 1	144 ± 1 #	149 ± 2 *
K^+, mM	4.1 ± 0.07	4.2 ± 0.13	4.9 ± 0.15 #	5.1 ± 0.19 #
Ca^{++}, mM	1.00 ± 0.01	1.13 ± 0.02 *	1.03 ± 0.01	1.05 ± 0.04
Hct, %	44 ± 1	44 ± 1	42 ± 1	42 ± 1
cHb, g dL^{-1}	14.6 ± 0.3	14.4 ± 0.2	14.0 ± 0.5	13.8 ± 0.4

Table 3: Densitometric analysis of the expression of ENaC subunits in kidney cortex from *nphs2$^{\Delta ipod}$*plg$^{+/+}$* and *nphs2$^{\Delta ipod}$*plg$^{-/-}$* mice before and after induction of nephrotic syndrome and under treatment with aprotinin

Signal intensity of the bands (relative units) was normalized for total protein expression of the respective lane.

Arithmetic means of expression in relative units ± SEM (n=4 each)

		uninduced		nephrotic + placebo		nephrotic + aprotinin	
	molecular weight, kDa	*nphs2$^{\Delta ipod}$*plg$^{+/+}$*	*nphs2$^{\Delta ipod}$*plg$^{-/-}$*	*nphs2$^{\Delta ipod}$*plg$^{+/+}$*	*nphs2$^{\Delta ipod}$*plg$^{-/-}$*	*nphs2$^{\Delta ipod}$*plg$^{+/+}$*	*nphs2$^{\Delta ipod}$*plg$^{-/-}$*
α-ENaC	87	186 ± 16	252 ± 23	229 ± 40	237 ± 29	223 ± 58	183 ± 75
	26	64 ± 12	90 ± 31	110 ± 11	98 ± 53	69 ± 3	95 ± 21
β-ENaC	85	8 ± 1	10 ± 1	8 ± 0.3	10 ± 1	11 ± 1	9 ± 1
γ-ENaC	84	178 ± 36	183 ± 45	142 ± 28	254 ± 37	284 ± 42	188 ± 23
	72	110 ± 9	163 ± 55	187 ± 24 #	141 ± 62	97 ± 13 §	133 ± 48

significant difference between uninduced and nephrotic mice of the same genotype (t-test), § significant difference between placebo and aprotinin-treated nephrotic mice (t-test).

Figure Legends

Figure 1. Deletion of podocin expression using an inducible Cre recombinase (tet-on) under a nephrin-driven promoter

(A) Scheme illustrating the involved alleles. Binding of doxycycline to the reverse tetracycline-controlled transactivator (rtTA) expressed under the nephrin promotor (Nefta8) leads to expression of a Cre recombinase and excision of a loxP-flanked region in the gene for podocin (nphs2).
(B) Podocin expression at the protein level in isolated glomeruli taken 14 days after end of induction with doxycycline
(C) Glomerular expression of podocin and nephrin as analyzed by immunofluorescence in kidney samples after 14 days. Note that in addition to the deletion of podocin, nephrin expression was also lost. Scale bar: 100 µm.
(D) Light microscopy of the same samples showing protein droplets (arrow) in dilated tubuli of nephrotic mice. Scale bar: 100 µm.
(E) Electron microscopy displayed normal foot processes in the uninduced animals (arrowheads) and foot process effacement indicated by (arrows) in the nephrotic mice. Scale bar: 2 µm.

Figure 2: Features of experimental nephrotic syndrome in *nphs2$^{\Delta ipod}$*plg$^{+/+}$* and *nphs2$^{\Delta ipod}$*plg$^{-/-}$* mice

(A) Course of urinary protein excretion after end of induction of experimental nephrotic syndrome.
(B-F) Plasma concentrations of albumin, cholesterol, urea, creatinine and aldosterone before and day 14.
(G) Western blot showing the expression of plasminogen and albumin in plasma (P) and urine (U) samples of *nphs2$^{\Delta ipod}$*plg$^{+/+}$* and *nphs2$^{\Delta ipod}$*plg$^{-/-}$* mice. Note that the nephrotic urine of *nphs2$^{\Delta ipod}$*plg$^{+/+}$* mice contains heavy chain of plasminogen at 80 kDa reflecting proteolytic activation by urokinase.
(H) Course of urinary and plasma plasmin(ogen) concentration in nephrotic *nphs2$^{\Delta ipod}$*plg$^{+/+}$* mice using an ELISA that detects both plasminogen zymogen and active plasmin.
(I) Course of urinary amidolytic activity against the chromogenic substrate S-2251 consisting of Val-Leu-Lys-p-Nitroaniline or VLK-pNA in *nphs2$^{\Delta ipod}$*plg$^{+/+}$* and *nphs2$^{\Delta ipod}$*plg$^{-/-}$* mice. This activity is strongly reduced in the absence of plasminogen (*nphs2$^{\Delta ipod}$*plg$^{-/-}$* mice).
Arithmetic means ± SEM, $^{\#}$ indicates significant difference to baseline value, * indicates significant difference between genotypes.

Figure 3. ENaC activation and sodium retention in nephrotic *nphs2$^{\Delta ipod}$*plg$^{+/+}$* and *nphs2$^{\Delta ipod}$*plg$^{-/-}$* mice

(A)Natriuretic response to vehicle (injectable water, 5 µl g^{-1} bw) or amiloride (10 µg g^{-1} bw i.p.). in uninduced and nephrotic *nphs2$^{\Delta ipod}$*plg$^{+/+}$* and *nphs2$^{\Delta ipod}$*plg$^{-/-}$* mice. Urine was collected for 6 h after injection and all mice underwent vehicle and amiloride injection sequentially (at day -21 and day 8, respectively). Mean values were 34 ± 7 and 26 ± 9 µmol 6 h^{-1} in uninduced *nphs2$^{\Delta ipod}$*plg$^{+/+}$* (n=10) and *nphs2$^{\Delta ipod}$*plg$^{-/-}$* mice (n=11) receiving vehicle and 93 ± 11 and 91 ± 11 µmol 6 h^{-1} receiving amiloride injection. In nephrotic *nphs2$^{\Delta ipod}$*plg$^{+/+}$* (n=9) and *nphs2$^{\Delta ipod}$*plg$^{-/-}$* mice (n=8) vehicle injection was followed by a significantly reduced urinary sodium excretion (3 ± 1 and 5 ± 1 µmol 6 h^{-1}, respectively). After amiloride injection urinary sodium excretion increased to 110 ± 26 and 159 ± 27 µmol 6 h^{-1}, respectively.

(B) Amiloride-sensitive natriuresis as the fold increase. In uninduced *nphs2$^{\Delta ipod}$*plg$^{+/+}$* and *nphs2$^{\Delta ipod}$*plg$^{-/-}$* mice this ratio was 4 ± 1 (n=10) and 9 ± 3 (n=11), respectively, in nephrotic *nphs2$^{\Delta ipod}$*plg$^{+/+}$* and *nphs2$^{\Delta ipod}$*plg$^{-/-}$* mice 72 ± 26 and 63 ± 16, respectively.

(C, D) Course of urinary sodium excretion in spot urine samples and body weight taken in the morning after induction of nephrotic syndrome in *nphs2$^{\Delta ipod}$*plg$^{+/+}$*, *nphs2$^{\Delta ipod}$*plg$^{-/-}$* mice and control mice, respectively.

Arithmetic means ± SEM, # indicates significant difference to baseline value, * indicates significant difference between genotypes, § indicates significant difference between uninduced and nephrotic state. A: amiloride; U: uninduced; N: nephrotic. V: vehicle.

Figure 4. Effect of the serine protease inhibitor aprotinin on sodium retention in nephrotic *nphs2$^{\Delta ipod}$*plg$^{+/+}$* and *nphs2$^{\Delta ipod}$*plg$^{-/-}$* mice

(A-E) Course of urinary aprotinin concentration, proteinuria, urinary amidolytic activity, sodium excretion and body weight after end of induction of nephrotic syndrome (day 0). Groups were separated after pellet implantation at day 3.

(F) Plasma concentration of aldosterone before and on day 8 after induction of nephrotic syndrome and implantation of a placebo or aprotinin pellet on day 4. Due to the large scatter there is no significant difference, however, the results are in line with the increase under the nephrotic state (Fig. 2F) and normalization under aprotinin treatment as described previously [4].

Arithmetic means ± SEM, # indicates significant difference to baseline value, * indicates significant difference between genotypes, § indicated significant difference between placebo and aprotinin-treated nephrotic mice. U: uninduced; N+P: nephrotic + placebo; N+A: nephrotic + aprotinin.

Figure 5. Expression of α-ENaC and γ-ENaC in kidney tissues from *nphs2$^{\Delta ipod}$*plg$^{+/+}$* and *nphs2$^{\Delta ipod}$*plg$^{-/-}$* mice.

Staining of α-ENaC (brown) and γ-ENaC using immunohistochemistry from formalin-fixed kidneys of uninduced, nephrotic and aprotinin-treated *nphs2$^{\Delta ipod}$*plg$^{+/+}$* and *nphs2$^{\Delta ipod}$*plg$^{-/-}$* mice. Kidneys were harvested at day 8 from the same mice as shown in Figure 4.

Figure 6. Expression of ENaC subunits in kidney cortex from *nphs2$^{\Delta ipod}$*plg$^{+/+}$* and *nphs2$^{\Delta ipod}$*plg$^{-/-}$* mice.

Western blots of proteins from membrane preparations of uninduced, nephrotic and aprotinin-treated *nphs2$^{\Delta ipod}$*plg$^{+/+}$* and *nphs2$^{\Delta ipod}$*plg$^{-/-}$* mice. Kidneys were harvested at day 8 from the same mice as shown in Figure 4 (each n=4). Results of application of the immunogenic peptide is shown in Supplemental Figure 4, results of quantification are shown in table 3. Corresponding plasma aldosterone concentrations are shown in Fig. 4F.

Figure 7. Current model of proteolytic ENaC activation in nephrotic syndrome

Glomerular proteinuria leads to aberrant filtration of serine proteases including uPA and plg as zymogens. Plg is activated by uPA leading to plasmin formation in the tubular space. However, this is not required for activation of ENaC by proteolysis of its γ-subunit. The identity of the essential serine protease(s) is not known.

Figure 1. Deletion of podocin expression using an inducible Cre recombinase (tet-on) under a nephrin-driven promoter

(A) Scheme illustrating the involved alleles. Binding of doxycycline to the reverse tetracycline-controlled transactivator (rtTA) expressed under the nephrin promotor (Nefta8) leads to expression of a Cre recombinase and excision of a loxP-flanked region in the gene for podocin (nphs2).
(B) Podocin expression at the protein level in isolated glomeruli taken 14 days after end of induction with doxycycline
(C) Glomerular expression of podocin and nephrin as analyzed by immunofluorescence in kidney samples after 14 days. Note that in addition to the deletion of podocin, nephrin expression was also lost. Scale bar: 100 µm.
(D) Light microscopy of the same samples showing protein droplets (arrow) in dilated tubuli of nephrotic mice. Scale bar: 100 µm.
(E) Electron microscopy displayed normal foot processes in the uninduced animals (arrowheads) and foot process effacement indicated by (arrows) in the nephrotic mice. Scale bar: 2 µm.

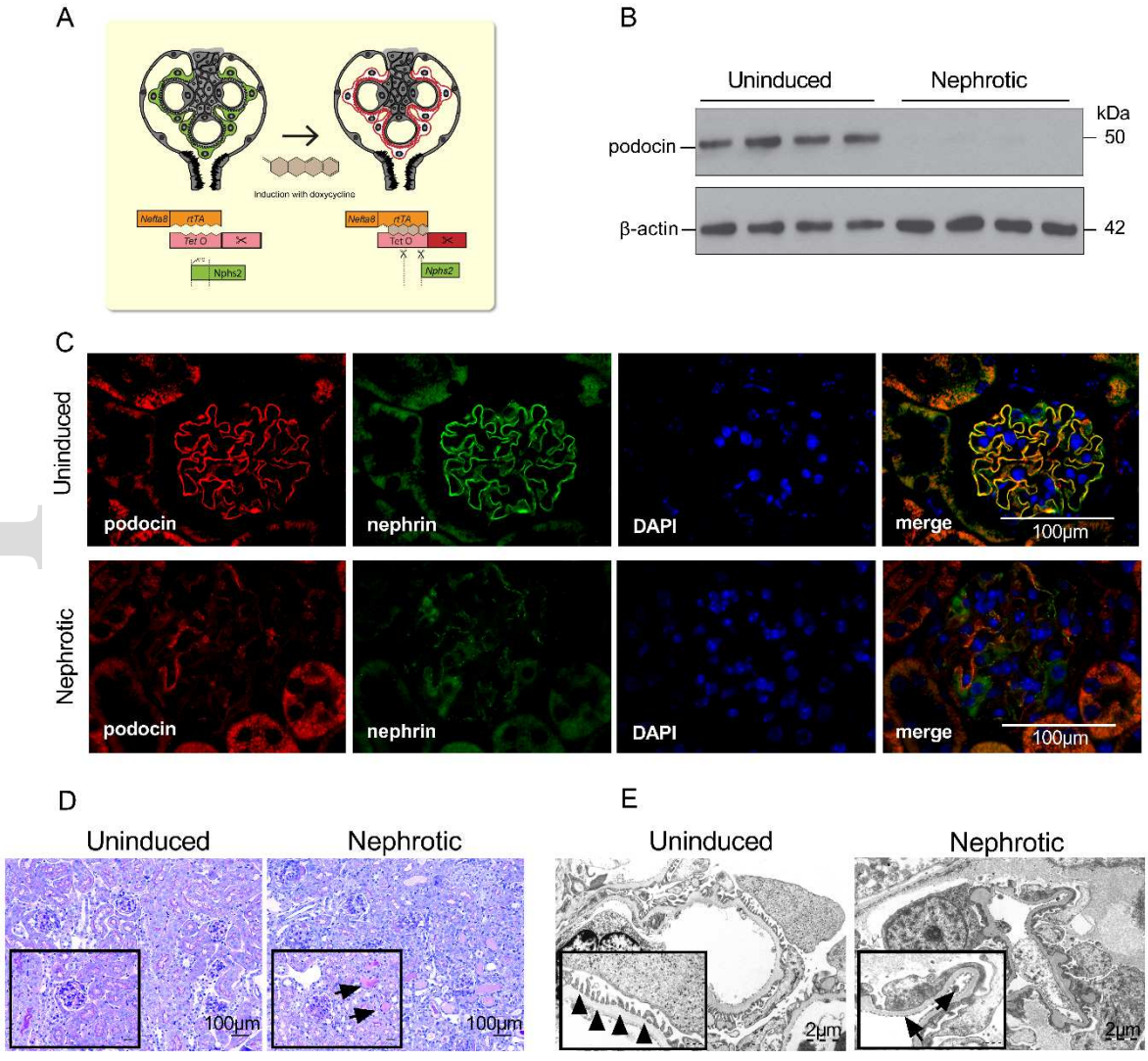

Figure 2: Features of experimental nephrotic syndrome in *nphs2$^{\Delta ipod}$*plg$^{+/+}$* and *nphs2$^{\Delta ipod}$*plg$^{-/-}$* mice

(A) Course of urinary protein excretion after end of induction of experimental nephrotic syndrome.
(B-F) Plasma concentrations of albumin, cholesterol, urea, creatinine and aldosterone before and day 14.
(G) Western blot showing the expression of plasminogen and albumin in plasma (P) and urine (U) samples of *nphs2$^{\Delta ipod}$*plg$^{+/+}$* and *nphs2$^{\Delta ipod}$*plg$^{-/-}$* mice. Note that the nephrotic urine of *nphs2$^{\Delta ipod}$*plg$^{+/+}$* mice contains heavy chain of plasminogen at 80 kDa reflecting proteolytic activation by urokinase.
(H) Course of urinary and plasma plasmin(ogen) concentration in nephrotic *nphs2$^{\Delta ipod}$*plg$^{+/+}$* mice using an ELISA that detects both plasminogen zymogen and active plasmin.
(I) Course of urinary amidolytic activity against the chromogenic substrate S-2251 consisting of Val-Leu-Lys-p-Nitroaniline or VLK-pNA in *nphs2$^{\Delta ipod}$*plg$^{+/+}$* and *nphs2$^{\Delta ipod}$*plg$^{-/-}$* mice. This activity is strongly reduced in the absence of plasminogen (*nphs2$^{\Delta ipod}$*plg$^{-/-}$* mice).

Arithmetic means ± SEM, # indicates significant difference to baseline value, * indicates significant difference between genotypes.

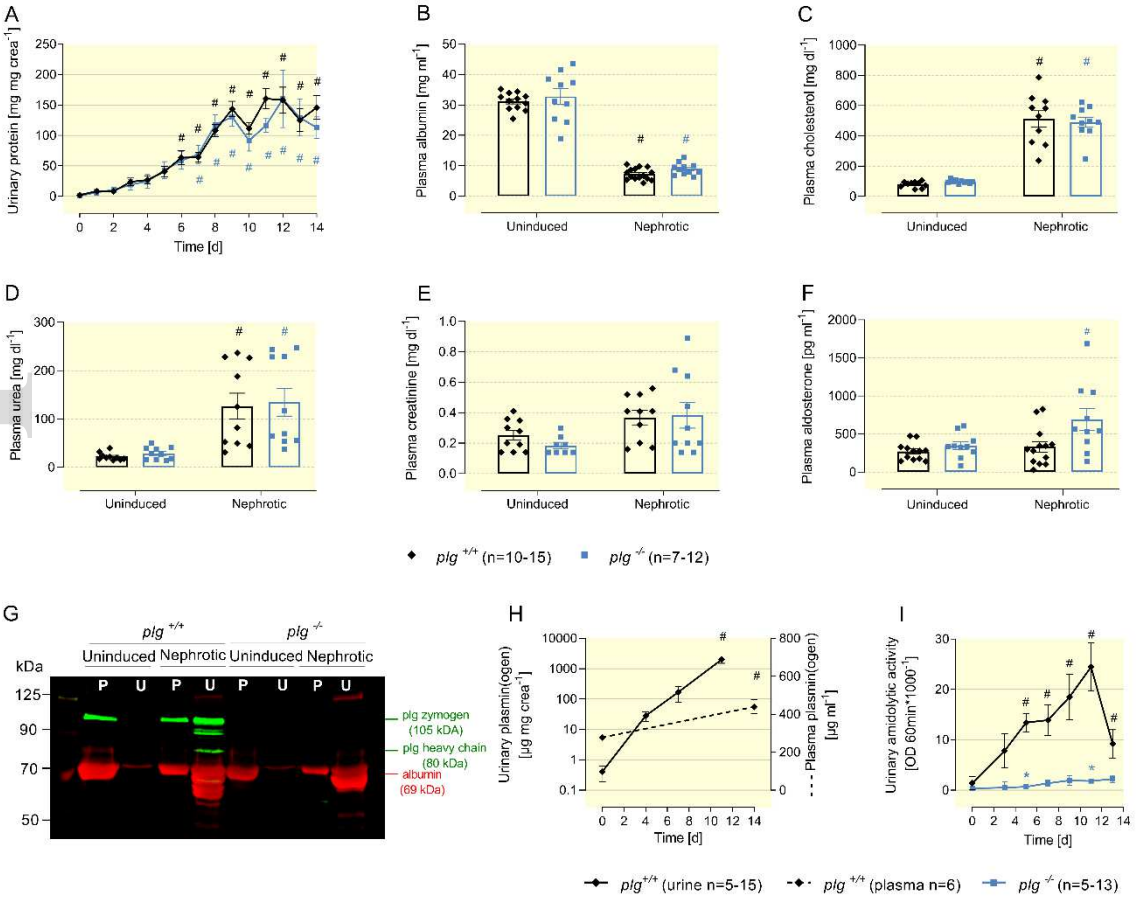

Figure 3. ENaC activation and sodium retention in nephrotic *nphs2$^{\Delta ipod}$*plg$^{+/+}$* and *nphs2$^{\Delta ipod}$*plg$^{-/-}$* mice

(A)Natriuretic response to vehicle (injectable water, 5 µl g^{-1} bw) or amiloride (10 µg g^{-1} bw i.p.). in uninduced and nephrotic *nphs2$^{\Delta ipod}$*plg$^{+/+}$* and *nphs2$^{\Delta ipod}$*plg$^{-/-}$* mice. Urine was collected for 6 h after injection and all mice underwent vehicle and amiloride injection sequentially (at day -21 and day 8, respectively). Mean values were 34 ± 7 and 26 ± 9 µmol 6 h^{-1} in uninduced *nphs2$^{\Delta ipod}$*plg$^{+/+}$* (n=10) and *nphs2$^{\Delta ipod}$*plg$^{-/-}$* mice (n=11) receiving vehicle and 93 ± 11 and 91 ± 11 µmol 6 h^{-1} receiving amiloride injection. In nephrotic *nphs2$^{\Delta ipod}$*plg$^{+/+}$* (n=9) and *nphs2$^{\Delta ipod}$*plg$^{-/-}$* mice (n=8) vehicle injection was followed by a significantly reduced urinary sodium excretion (3 ± 1 and 5 ± 1 µmol 6 h^{-1}, respectively). After amiloride injection urinary sodium excretion increased to 110 ± 26 and 159 ± 27 µmol 6 h^{-1}, respectively.

(B) Amiloride-sensitive natriuresis as the fold increase. In uninduced *nphs2$^{\Delta ipod}$*plg$^{+/+}$* and *nphs2$^{\Delta ipod}$*plg$^{-/-}$* mice this ratio was 4 ± 1 (n=10) and 9 ± 3 (n=11), respectively, in nephrotic *nphs2$^{\Delta ipod}$*plg$^{+/+}$* and *nphs2$^{\Delta ipod}$*plg$^{-/-}$* mice 72 ± 26 and 63 ± 16, respectively.

(C, D) Course of urinary sodium excretion in spot urine samples and body weight taken in the morning after induction of nephrotic syndrome in *nphs2$^{\Delta ipod}$*plg$^{+/+}$*, *nphs2$^{\Delta ipod}$*plg$^{-/-}$* mice and control mice, respectively.

Arithmetic means ± SEM, $^{\#}$ indicates significant difference to baseline value, * indicates significant difference between genotypes, § indicates significant difference between uninduced and nephrotic state. A: amiloride; U: uninduced; N: nephrotic. V: vehicle.

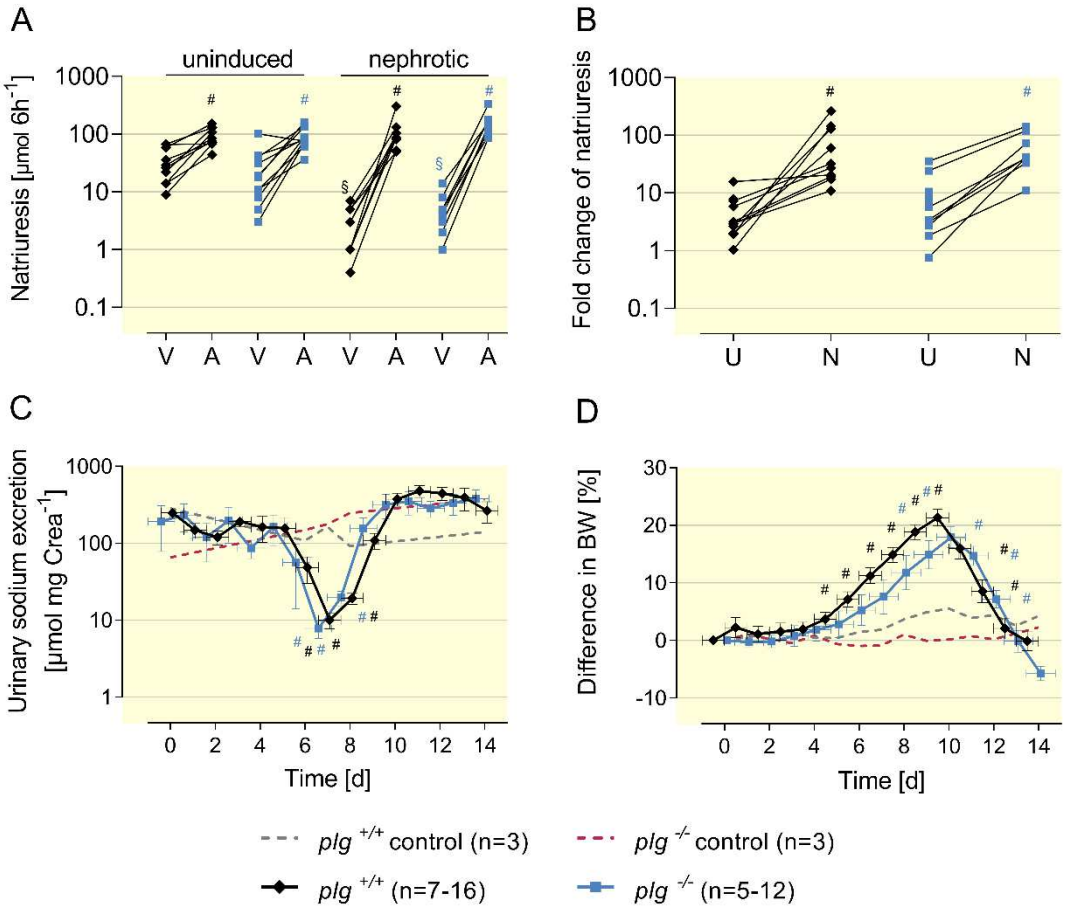

Figure 4. Effect of the serine protease inhibitor aprotinin on sodium retention in nephrotic *nphs2*$^{\Delta ipod}$plg*$^{+/+}$ and *nphs2*$^{\Delta ipod}$**plg*$^{-/-}$ mice**

(A-E) Course of urinary aprotinin concentration, proteinuria, urinary amidolytic activity, sodium excretion and body weight after end of induction of nephrotic syndrome (day 0). Groups were separated after pellet implantation at day 3.

(F) Plasma concentration of aldosterone before and on day 8 after induction of nephrotic syndrome and implantation of a placebo or aprotinin pellet on day 4. Due to the large scatter there is no significant difference, however, the results are in line with the increase under the nephrotic state (Fig. 2F) and normalization under aprotinin treatment as described previously [4].

Arithmetic means ± SEM, # indicates significant difference to baseline value, * indicates significant difference between genotypes, § indicated significant difference between placebo and aprotinin-treated nephrotic mice. U: uninduced; N+P: nephrotic + placebo; N+A: nephrotic + aprotinin.

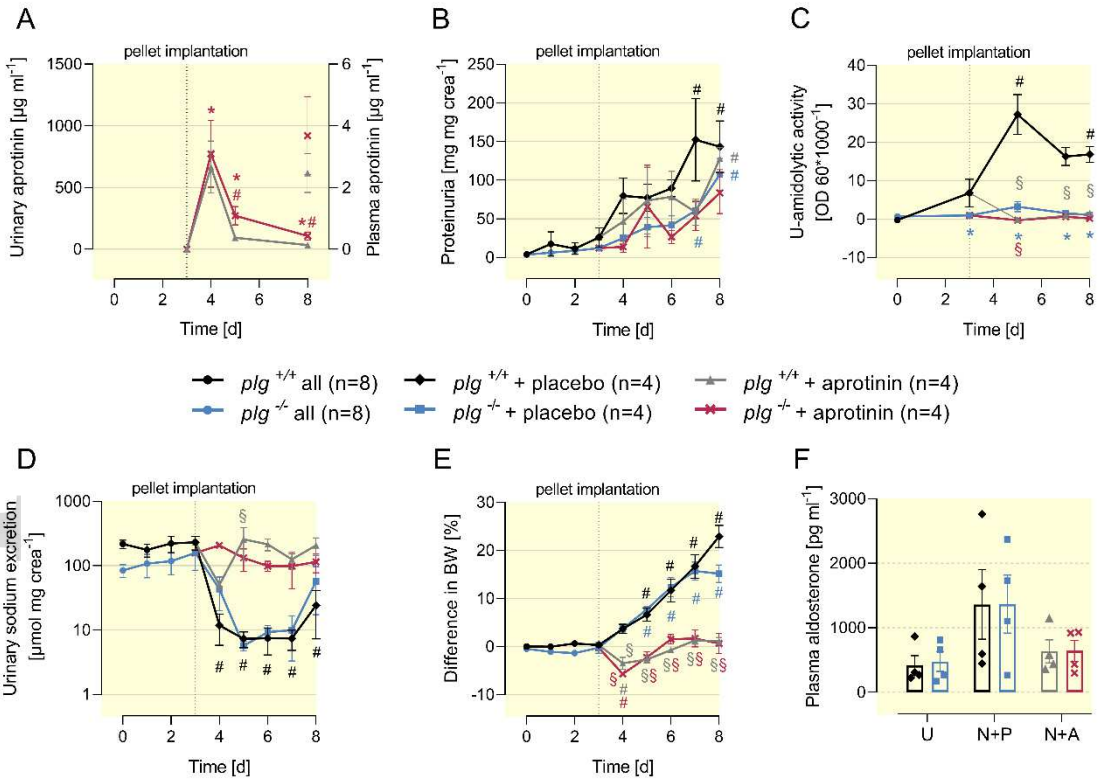

Figure 5. Expression of α-ENaC and γ-ENaC in kidney tissues from *nphs2*$^{\Delta ipod}$plg*$^{+/+}$ and *nphs2*$^{\Delta ipod}$**plg*$^{-/-}$ mice.**

Staining of α-ENaC (brown) and γ-ENaC using immunohistochemistry from formalin-fixed kidneys of uninduced, nephrotic and aprotinin-treated *nphs2*$^{\Delta ipod}$**plg*$^{+/+}$ and *nphs2*$^{\Delta ipod}$**plg*$^{-/-}$ mice. Kidneys were harvested at day 8 from the same mice as shown in Figure 4.

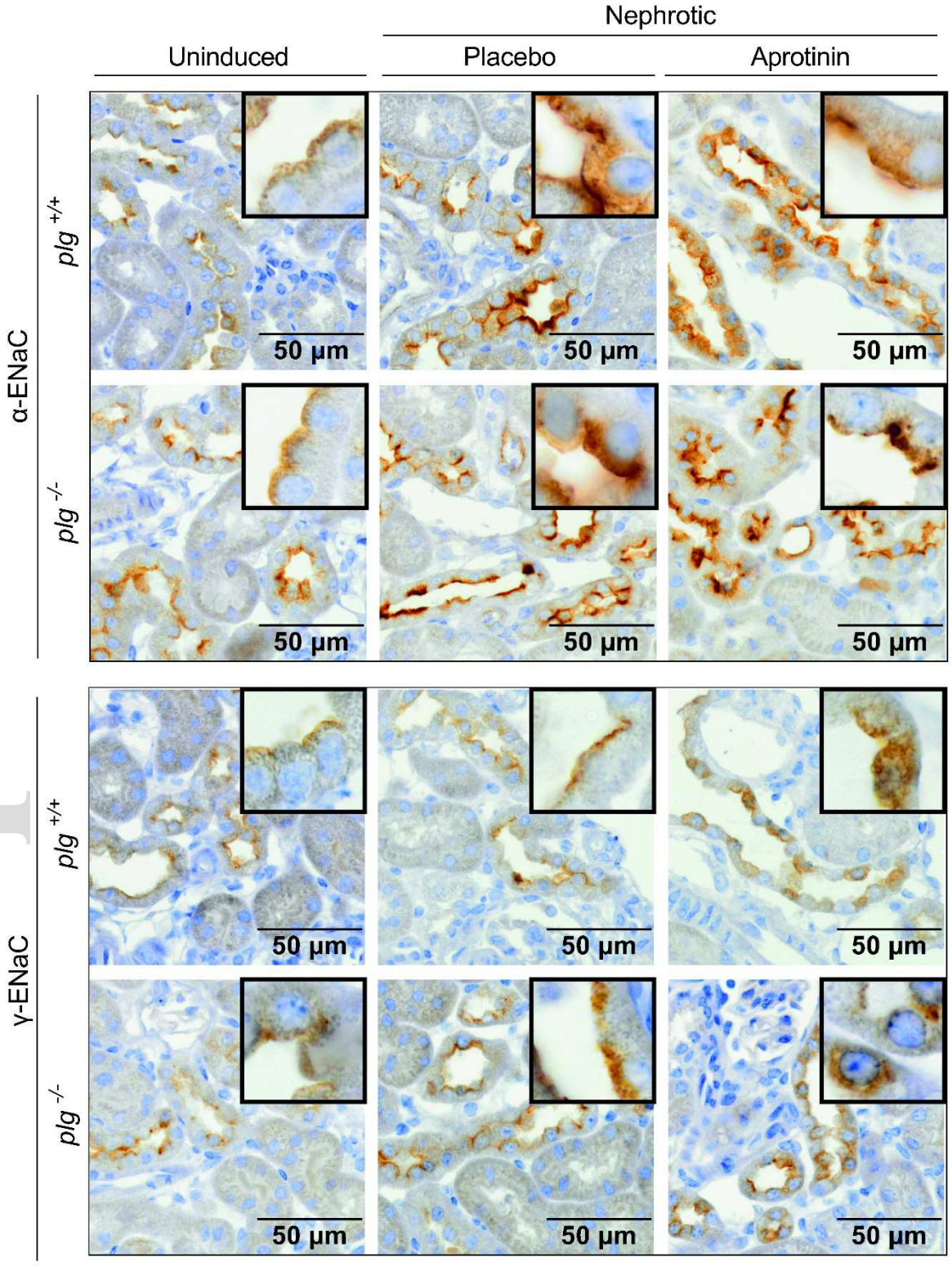

Figure 6. Expression of ENaC subunits in kidney cortex from *nphs2*$^{\Delta ipod}$plg*$^{+/+}$ and *nphs2*$^{\Delta ipod}$**plg*$^{-/-}$ mice.**

Western blots of proteins from membrane preparations of uninduced, nephrotic and aprotinin-treated *nphs2*$^{\Delta ipod}$**plg*$^{+/+}$ and *nphs2*$^{\Delta ipod}$**plg*$^{-/-}$ mice. Kidneys were harvested at day 8 from the same mice as shown in Figure 4 (each n=4). Results of application of the immunogenic peptide is shown in Supplemental Figure 4, results of quantification are shown in table 3. Corresponding plasma aldosterone concentrations are shown in Fig. 4F.

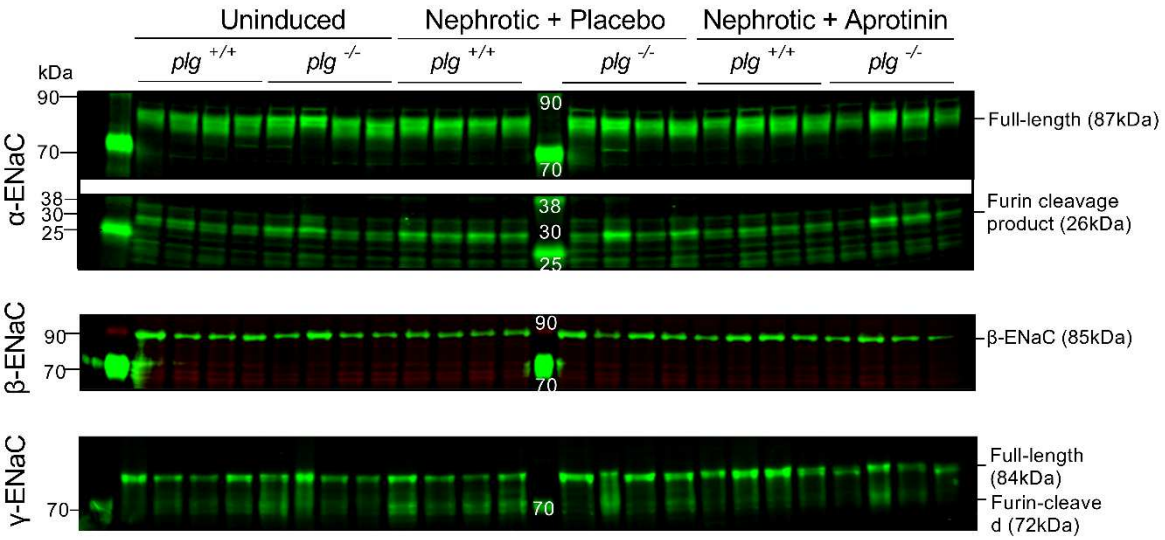

Figure 7. Current model of proteolytic ENaC activation in nephrotic syndrome

Glomerular proteinuria leads to aberrant filtration of serine proteases including uPA and plg as zymogens. Plg is activated by uPA leading to plasmin formation in the tubular space. However, this is not required for activation of ENaC by proteolysis of its γ-subunit. The identity of the essential serine protease(s) is not known.